MIT Joint Program on the Science and Policy of Global Change

Relative Roles of Climate Sensitivity and Forcing in Defining the Ocean Circulation Response to Climate Change

Jeffery R. Scott, Andrei P. Sokolov, Peter H. Stone and Mort D. Webster

Report No. 148
May 2007

The MIT Joint Program on the Science and Policy of Global Change is an organization for research, independent policy analysis, and public education in global environmental change. It seeks to provide leadership in understanding scientific, economic, and ecological aspects of this difficult issue, and combining them into policy assessments that serve the needs of ongoing national and international discussions. To this end, the Program brings together an interdisciplinary group from two established research centers at MIT: the Center for Global Change Science (CGCS) and the Center for Energy and Environmental Policy Research (CEEPR). These two centers bridge many key areas of the needed intellectual work, and additional essential areas are covered by other MIT departments, by collaboration with the Ecosystems Center of the Marine Biology Laboratory (MBL) at Woods Hole, and by short- and long-term visitors to the Program. The Program involves sponsorship and active participation by industry, government, and non-profit organizations.

To inform processes of policy development and implementation, climate change research needs to focus on improving the prediction of those variables that are most relevant to economic, social, and environmental effects. In turn, the greenhouse gas and atmospheric aerosol assumptions underlying climate analysis need to be related to the economic, technological, and political forces that drive emissions, and to the results of international agreements and mitigation. Further, assessments of possible societal and ecosystem impacts, and analysis of mitigation strategies, need to be based on realistic evaluation of the uncertainties of climate science.

This report is one of a series intended to communicate research results and improve public understanding of climate issues, thereby contributing to informed debate about the climate issue, the uncertainties, and the economic and social implications of policy alternatives. Titles in the Report Series to date are listed on the inside back cover.

Henry D. Jacoby and Ronald G. Prinn,
Program Co-Directors

For more information, please contact the Joint Program Office

Postal Address: Joint Program on the Science and Policy of Global Change
77 Massachusetts Avenue
MIT E40-428
Cambridge MA 02139-4307 (USA)

Location: One Amherst Street, Cambridge
Building E40, Room 428
Massachusetts Institute of Technology

Access: Phone: (617) 253-7492
Fax: (617) 253-9845
E-mail: globalchange@mit.edu
Web site: http://MIT.EDU/globalchange/

Printed on recycled pape

Relative Roles of Climate Sensitivity and Forcing in Defining the Ocean Circulation Response to Climate Change

Jeffery R. Scott, Andrei P. Sokolov, Peter H. Stone, and Mort D. Webster

Abstract

The response of the ocean's meridional overturning circulation (MOC) to increased greenhouse gas forcing is examined using a coupled model of intermediate complexity, including a dynamic 3D ocean subcomponent. Parameters are the increase in CO_2 forcing (with stabilization after a specified time interval) and the model's climate sensitivity. In this model, the cessation of deep sinking in the north "Atlantic" (hereinafter, a "collapse"), as indicated by changes in the MOC, behaves like a simple bifurcation. The final surface air temperature (SAT) change, which is closely predicted by the product of the radiative forcing and the climate sensitivity, determines whether a collapse occurs. The initial transient response in SAT is largely a function of the forcing increase, with higher sensitivity runs exhibiting delayed behavior; accordingly, high CO_2-low sensitivity scenarios can be assessed as a recovering or collapsing circulation shortly after stabilization, whereas low CO_2-high sensitivity scenarios require several hundred additional years to make such a determination. We also systemically examine how the rate of forcing, for a given CO_2 stabilization, affects the ocean response. In contrast with previous studies based on results using simpler ocean models, we find that except for a narrow range of marginally stable to marginally unstable scenarios, the forcing rate has little impact on whether the run collapses or recovers. In this narrow range, however, forcing increases on a time scale of slow ocean advective processes results in weaker declines in overturning strength and can permit a run to recover that would otherwise collapse.

Contents

1. INTRODUCTION

The behavior of the climate system in response to changes in greenhouse gases strongly depends on two critical variables: changes in greenhouse gas levels and the sensitivity of the climate system to these imposed changes. Both these variables are highly uncertain. The rate of increase in greenhouse gases is a function of both anthropogenic changes in emissions and the climate system's ability to sequester these increases. Projections of future emissions are based on assumptions of economic and population growth, technological change, and the effectiveness of potential regulation of emissions. The latter is often implicit in greenhouse gas "stabilization" scenarios, which explore the longer-term climate response to holding concentrations constant once they reach a predetermined level. Climate sensitivity of a coupled model is a function of the physics and parameterizations used in the respective subcomponent models (Meehl *et al*., 2004), and also likely depends on coupling procedures used to link these subcomponents (Marotzke and

Stone, 1995). This results in significant differences in climate sensitivities between existing climate models (Cubasch *et al.,* 2001; Colman, 2003). Climate change observed in the 20th century also can only place limited constraints on this quantity (Andronova and Schlesinger, 2001; Gregory *et al.*, 2002; Forest *et al.*, 2002; Forest *et al*., 2006). Improvements in climate models are expected with gains in computational resources, but will also require improvements in our understanding and representation of physical processes. Even with such expected improvements, however, significant uncertainty in these parameters will remain.

We examine the response of a coupled climate model given different greenhouse gas forcings and climate sensitivities. The former is accomplished through different prescribed increases in CO_2 concentration in the atmospheric sub-model, the latter by varying the cloud response to changes in surface temperature (Sokolov and Stone, 1998). We are particularly interested in the behavior of the model's meridional overturning circulation (MOC). The MOC plays a significant role as a conveyor of heat and tracers throughout the ocean, and in particular contributes a sizeable northward heat transport in the Atlantic Ocean (Ganachaud and Wunsch, 2000). Typical coupled model runs show a gradual weakening of the Atlantic MOC, in response to an increase in radiative forcing (Cubasch *et al.*, 2001; Gregory *et al*., 2005), although there is a considerable variation across models in the magnitude of this weakening. A complete model description, including discussion of our model's response to enhanced greenhouse gas forcing as compared with other coupled models, is presented in section 2.

In section 3, we have carried out over 60 climate change simulations, effectively covering a plausible portion of phase space, by varying these two "parameters" (*i.e.* CO_2 concentration and climate sensitivity) in the model. Ranges for climate sensitivity and radiative forcing were based on the results of Forest *et al*. (2002) and Webster *et al*. (2002). A novel aspect of this work is that we are interested in the interaction of these parameters across a full range of conceivable climate responses to global warming, particularly when the climate state is near a bifurcation. In our simulations, we examine the climate response as the global ocean circulation weakens and recovers, or in some cases, collapses, looking at a 1000-year (or longer) time horizon (as previously noted, a "collapse" being defined as a shutdown of deep convection and net downwelling in the North Atlantic).

Using an annual mean, energy balance atmospheric model coupled to a zonally-averaged three-basin ocean model, Stocker and Schmittner (1997, hereinafter SS97; see also Schmittner and Stocker, 1999) studied the atmospheric CO_2 level required for ocean circulation collapse and how it depends on the rate of CO_2 increase and climate sensitivity, similar to this study. A major result was that the ocean circulation was considerably less stable given a more rapid increase to a specified level of CO_2. Their array of experiments exploring the possibility of collapse across a range of forcings and climate sensitivities is similar to ours, yet there is a subtle difference. Their forcing increases occurred for variable lengths of time, until a desired final level of CO_2 was reached (the minimum level necessary to collapse the circulation is contoured on their Figure 4). In our comparable experiments in section 3 of this paper, CO_2 was held constant after 100 years of increase, with different rates of increase occurring during this period. In other words, we examine the ocean stability for a "stabilization scenario" occurring at a specific point in time, rather than stabilization occurring at a predetermined level of CO_2. In section 4, we specifically examine the impact of the forcing rate, given identical final CO_2 levels, in the context of the results from section 3. Thus, we more generally investigate how the rate of forcing affects the ocean response; this question was also addressed in Stouffer and Manabe (1999, hereinafter SM99) using fully coupled three-dimensional (3D) atmosphere-ocean models, although their runs were of shorter duration, using a single climate sensitivity.

Our use of a 3D ocean model represents a significant step forward as compared to a zonally-averaged model in examining ocean circulation stability. The MOC is governed by thermal wind balance; this balance is fundamentally three-dimensional, and other processes that play a role (such as parameterized eddy dynamics and convective adjustment) can also have important zonal structure. It has been previously argued that zonally-averaged models are problematic for MOC study (Marotzke and Scott, 1999). Important features of the ocean circulation found in 3D models, such as zonal circulations and gyre circulations, are entirely absent. The reader is referred to Wright *et al.* (1998) for a more complete discussion of two-dimensional (2D) ocean circulation models and their inherent assumptions and limitations. On the other hand, several studies suggest that the stability behavior of 2D models adequately mimics 3D general circulation model (GCM) studies (*e.g.*, Weijer and Dijkstra, 2001). Our goal is to revisit SS97's results taken to the next level of model complexity; our results will strongly suggest that the use of 2D ocean models for transient global warming experiments is dubious. In addition to 3D ocean dynamics, other important improvements here include the addition of the seasonal cycle, a (2D) freshwater forcing field based on actual observations, the addition of dynamics, radiation, and cloud processes in the atmospheric model, and inclusion of the Arctic Ocean (which is a critical component of our collapse mechanism).

We conclude with discussion and summary of results in section 5.

2. MODEL DESCRIPTION

The principle subcomponents of the model are as follows:

Atmosphere: The atmospheric model (Sokolov and Stone, 1998) is a zonally-averaged statistical-dynamical model developed from the GISS GCM Model II (Hansen *et al*., 1983). The resolution of the model is 4 degrees in latitude with 11 vertical layers. The model solves the zonally-averaged primitive equations with parameterizations of the main physical processes, including eddy transports of heat, moisture, and momentum, clouds, convection, and radiation. Four different allowable surface-types affect the surface fluxes, specifically ocean, land, sea-ice, and land-ice, with the terrestrial hydrography provided by a simple two-layer "bucket" model. The atmosphere's internal time step is 10 minutes.

Ocean: The ocean model is based on the MIT ocean general circulation model (Marshall *et al*., 1997). The bathymetry used here (**Figure 1**) consists of interconnected rectangular, flat-bottom ocean basins (our "Indian", "Pacific", and "Atlantic" oceans), with topographic sills in our "Indonesian Passage", "Drake Passage" and in the "Labrador Sea" and "Greenland Sea"

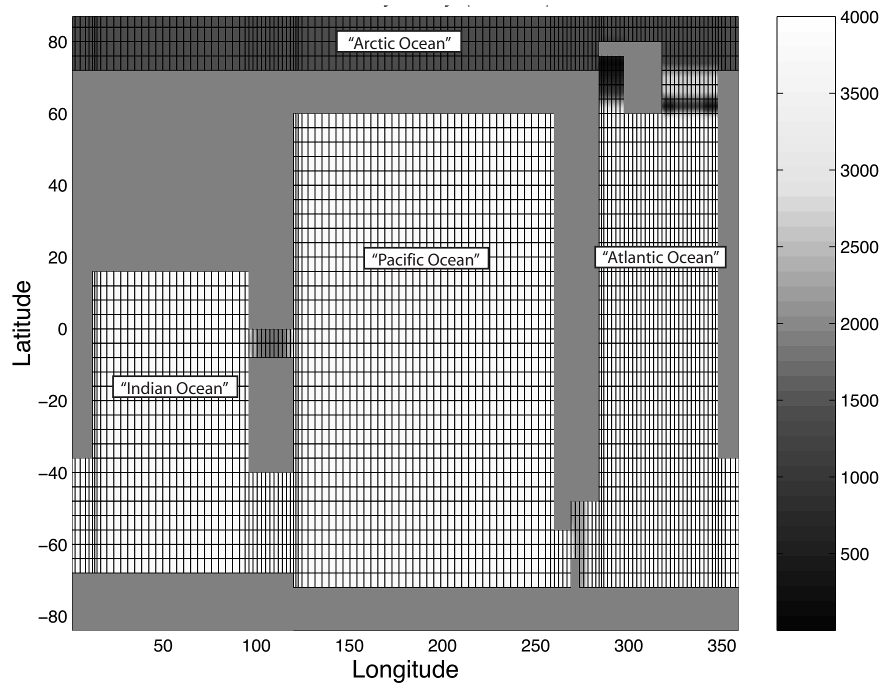

Figure 1. Ocean model bathymetry in meters, overlaid by ocean model grid. Note the decreased zonal grid spacing near the boundaries, which allows for improved resolution of the boundary currents. Ocean basins are labeled to provide a reference to crudely similar ocean basins on Earth.

regions. The model also includes a flat-bottom "Arctic Ocean", albeit considerably more shallow than the other oceans. Resolution with latitude is uniform at 4º, while resolution with longitude is enhanced near boundary currents, which improves the model's fidelity of ocean heat transport (Kamenkovich *et al*., 2000). The ocean model employs the Gent-McWilliams (1990) and Redi (1982) parameterizations of the effect of mesoscale eddies on isopycnals; diapycnal mixing in the model is represented using a prescribed uniform vertical diffusivity of 0.3 $cm^2\ s^{-1}$.

Sea-Ice: The model includes a 3-layer thermodynamic sea-ice model, as described in Winton (2000) and Bitz and Lipscombe (1999).

Coupling/Air-Sea Exchange: The model uses flux adjustments of zonal wind stress, heat, and freshwater between the oceanic and atmospheric sub-models. In the spin-up phase, temperature was restored in the surface layer (90-day timescale) using a "mapping" of zonally-averaged, monthly-mean Levitus and Boyer (1994) climatology for each ocean basin: maintaining this zonal average, a linear trend across each basin was applied to the target temperature by comparing the actual temperature in the western sector vs. the zonal average. Similarly, a linear trend was applied to the zonal mean freshwater forcing field (see **Figure 2**) based on the Jiang *et al*. (1999) data set. In order to improve upon the resulting surface model salinity as compared with the Levitus and Boyer climatology, the resulting data set was then modified slightly to freshen the tropical and northern Atlantic and increase salinity in the Pacific (given the idealized geometry and large uncertainty/error in the observed evaporation field, some modification of the Jiang *et al*. field was not only reasonable, but unavoidable). A final modification was the addition of 0.05 Sv to the freshwater input into the Arctic (co-located with

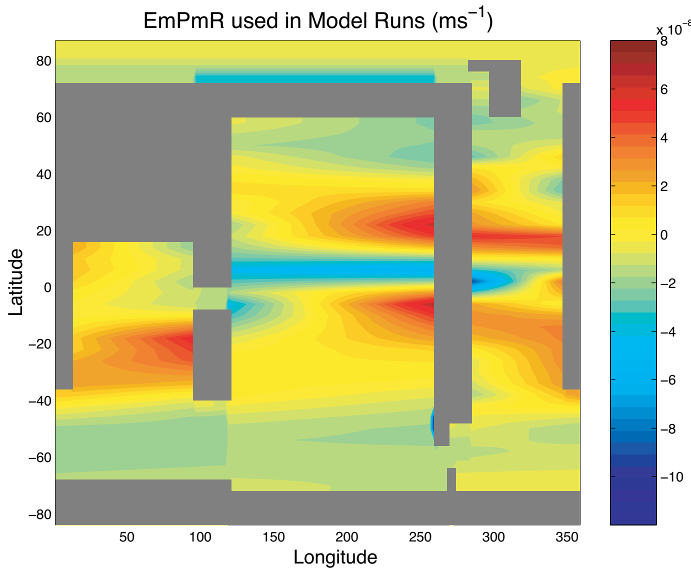

Figure 2. Freshwater forcing field (evaporation minus precipitation minus runoff) used to force the ocean mixed layer in the model's present-day state. For transient experiments, flux adjustments are diagnosed from the model spin-up, so that the ocean effectively receives this field plus any anomalies in freshwater forcing resulting from changing atmospheric CO_2 concentration.

anomalous river runoff in our transient experiments, as specified below), which served to further weaken the overturning and thus bring the circulation closer to the bifurcation point. The final surface freshwater fluxes were then applied to the ocean/sea-ice surface without any salinity restoring.

All told, these modifications weakened the maximum overturning in the North Atlantic from 23 Sv to 12 Sv, The original overturning was well above the observed estimates for the present-day circulation of approximately 15-18 Sv (Ganachaud and Wunsch, 2000; Talley *et al.*, 2003), whereas the weakened overturning is slightly less than estimated. The MIT-UW model (Kamenkovich *et al*., 2002), a predecessor of this model, also used the Jiang *et al.,* freshwater forcing data, although without such modifications; the hysteresis curve of that model (**Figure 3**) showed it to be significantly more stable than all other intermediate complexity models described in Rahmstorf *et al.* (2005), whereas the hysteresis curve of the model used here is now very typical of the rest. Zonal wind stresses were generated by taking zonal averages for each ocean basin based on the Trenberth *et al.* (1989) climatology, without applying any linear trend across the basin. Following the spin-up phase, flux adjustments of heat and freshwater are computed and used to equilibrate the "fully-coupled" model; the technique of anomaly coupling is employed for the zonal wind field. The meridional wind stress applied to the ocean surface is coupled directly from the 2D atmospheric model. Coupling between the atmosphere and ocean/sea-ice model occurs every four hours, which is the ocean model's time step for advecting tracers. Further detail on the general coupled model can be found in Dutkiewicz *et al*. (2005).

Our model's open passage through our idealized "Canadian Archipelago" plays an important role in the increased CO_2 simulations. It has been observed that the Arctic runoff has increased roughly 7% over the last sixty years (Peterson *et al*., 2002) and coupled climate model results

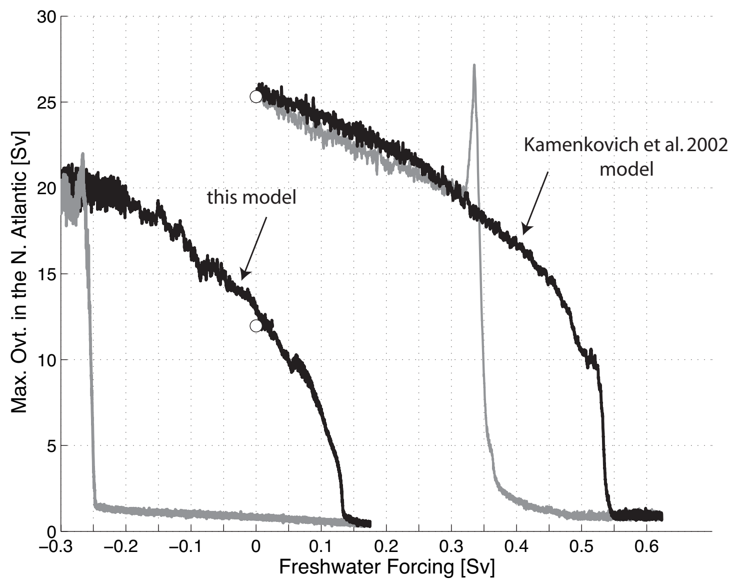

Figure 3. Hystersis curve comparison between this model and the model used in Kamenkovich *et al.* (2002). The starting points of the models' integration, *i.e.* the model's control present-day climate, are denoted by hollow circles. In the Rahmstorf *et al.* (2005) model intercomparison (see their Figure 2), four of the six models with "realistic" 3D ocean models and three out of five with "simplified" ocean models placed the present-day state near the middle of the hysteresis loop, similar to our model above. The width of our hysteresis loop is larger than those within the Rahmstorf *et al.* "realistic" group, but more similar to many in the "simplified" ocean group (Rahmstorf *et al.* choose to group the Kamenkovich *et al.* model in the "simplified" group, since their ocean basins were rectangular, even more simplified than the topography employed here). Also note that the streamfunction here and in Kamenkovich *et al.* remain slightly non-zero even with a collapsed circulation; this small value is from the wind-driven Ekman cell in the Northern Hemisphere.

suggest this trend will continue, if not increase (Wu *et al*., 2005). Previous ocean model studies have shown that the MOC is indeed quite sensitive to increasing Arctic discharge (Goosse *et al.,* 1997; Otterå *et al*., 2004; Peltier *et al.,* 2006; Rennermalm *et al*., 2006) although the degree of this sensitivity appears to be model dependent. Our model employs a flexible river-routing scheme for anomalous runoff (as calculated in the atmospheric subcomponent). In the southern hemisphere, for simplicity (and lacking a river network in this idealized topography) this runoff is distributed evenly over all ocean points. In the northern hemisphere, however, all anomalous runoff is diverted to the Arctic Ocean at 72-76°N between 96° and 260° in longitude. A comparison of our model's anomalous freshwater and surface heat (given a 1% increase in CO_2 for 70 years) with several models in the Coupled Model Intercomparison Project (as shown in Huang *et al.,* 2003 Figure 1) suggests that our model is fairly typical in its atmospheric response. As such, the diversion of anomalous runoff was necessary in order to achieve a collapse in ocean circulation across a sizeable portion of our parameter phase space. Given this and other model idealizations, our model cannot be expected to give realistic information about when a collapse will occur. Rather, our goal is to study qualitatively how the collapse depends on the parameters, and our anomalous runoff routing scheme allows us to do so in a realistic parameter range.

For our climate change scenarios in section 3, the level of atmospheric CO_2 is increased at different compound rates for 100 years and then held constant at the resulting level. Thus, the final level of CO_2 in the atmosphere is dictated by the rate of increase, with the resulting radiative forcing linearly proportional to the rate. Values of climate sensitivity shown throughout the paper represent an equilibrium sensitivity of the atmospheric model coupled to a mixed layer ocean model for a doubling of CO_2 concentration. A lookup table was created to equate our cloud feedback coefficient to specific mixed layer model climate sensitivity. However, defined in such a way, climate sensitivity does not exactly match the climate sensitivity of the coupled climate model because of interaction between the atmosphere and the dynamic ocean, with the disparity as large as 0.5 °C in several of the experiments.

3. STABILIZATION EXPERIMENTS WITH 100-YEAR FORCING PERIOD

Parameter phase space is presented in **Figure 4**, with symbols representing individual runs. Changes in global annual mean surface air temperature (SAT) for runs plotted using black symbols are shown in **Figure 5**a. A time series of the maximum North Atlantic meridional overturning streamfunction for these runs is plotted in Figure 5b. Note that this subset includes several runs with identical sensitivity and several runs with identical CO_2 increases.

In the first 100 years, when the largest changes in SAT occur, the initial rate of increase in SAT is roughly proportional to the rate of CO_2 increase. During this period, the effect of sensitivity on SAT is relatively minor. In years 100-300, however, SAT increases more rapidly in higher sensitivity runs, with only modest further increase in runs with low sensitivity. This

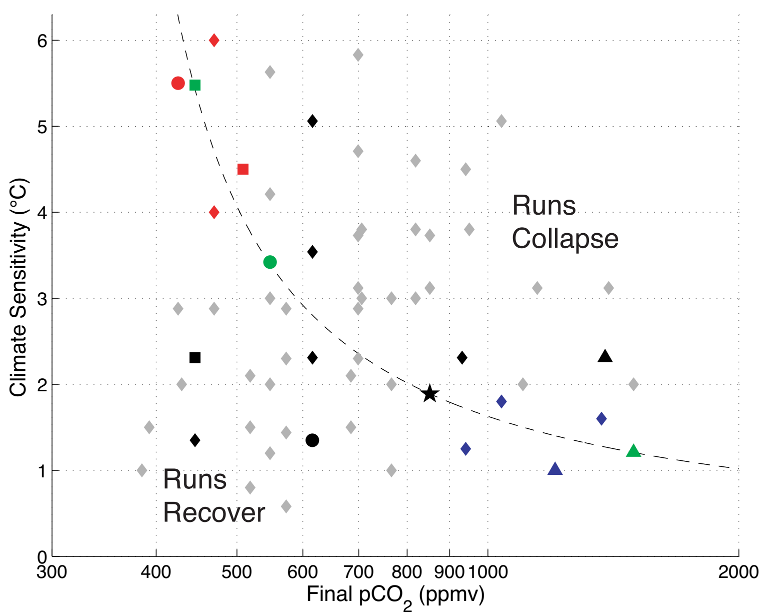

Figure 4. Phase space of all model runs forced by increasing CO_2 for 100 years (at a constant percent increase) and held constant at the 100-yr level thereafter. Runs in black are presented in Figure 5; runs in blue and red are presented in Figure 6. The dashed line is a plot of constant Log(C/315 ppmv)*S, where C is the final CO_2 concentration and S is climate sensitivity. A reference point on this line was the 852 ppmv/1.9 °C run (*i.e.* through the black star above), and to close approximation this line demarcates the regions of THC recovery (lower left) and collapse (upper right).

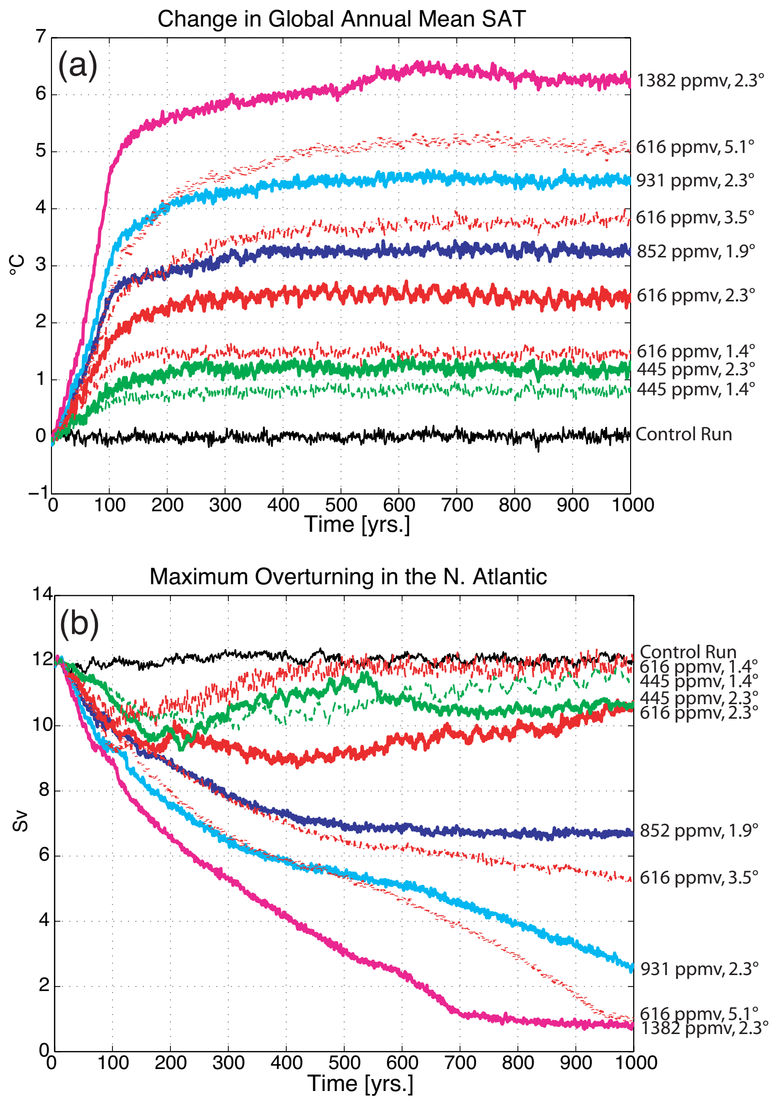

Figures 5. Results for runs with forcings given by the black symbols in Figure 4, as compared to a control run. CO_2 concentration at year 100 (and thereafter) and climate sensitivity is labeled to the right of the respective time series: **(a)** change in global annual mean SAT; **(b)** maximum overturning streamfunction in the North Atlantic.

behavior of the high sensitivity runs is qualitatively similar in SM99's greenhouse gas forcing experiments, where only a percentage of the equilibrium increase in SAT was achieved at the point of doubling CO_2, particularly when it occurred in less than 100 years (their model's climate sensitivity was 4.5°C, which falls in the range of our "high sensitivity" scenarios). Since the time scale for the atmospheric response to changes in radiative forcing is relatively short, the slower response in high sensitivity runs is due to delay in the amplification of climate feedbacks (Hansen *et al.*, 1985; Raper *et al.*, 2002). The subduction of heat below the ocean surface attenuates the increase in SAT, which effectively delays the full impact of all temperature-dependent feedbacks. Except for the two time series with greatest increase in SAT, the runs plotted in Figure 5a seem quite close to equilibration after 500 years.

As a consequence of the increase in SAT, the increase of Arctic runoff at year 100 ranges from 0.03 to 0.10 Sv, which as discussed has important consequences for the ocean circulation. A 0.10 Sv increase is roughly a doubling of the current real-world Arctic runoff; the lower half of the range is more plausible, however, as it is comparable to the Wu *et al.* (2005) projections using the HadCM3 climate model (note that Wu *et al.*'s time series of Arctic runoff, as shown in their Figure 4, ends at year 2050, so some extrapolation is necessary to estimate a 100-yr change). In Figure 5b, it is immediately clear that several of the runs are headed toward a collapse of the North Atlantic overturning circulation, while others weaken initially and then recover and/or are in the process of recovering. Unlike SAT, the meridional overturning circulation is not yet at equilibrium after 1000 years in most simulations. This slow response is due primarily to the long equilibration timescale of the deep ocean. Somewhat surprisingly, however, in our runs the global mean ocean temperature (not shown) has achieved a large percentage of its CO_2-related warming by 1000 years. In SM99, a timescale of several thousand years is necessary for deep ocean equilibration, which suggests ocean heat uptake is more efficient in our model.

At increased CO_2 levels, the strength of the overturning at equilibrium (requiring somewhat longer integration than plotted here; see Figures 9-12) is only modestly weaker in those runs that recover, despite significant warming. Stouffer and Manabe (2003) observed similar results using their coupled model. Wiebe and Weaver (1999), using an energy balance model coupled to an ocean GCM, found considerably larger overturning with CO_2 increases. In contrast, SS97's overturning recovery was to a decidedly weaker state than our model, although it should be noted that their control-state overturning was considerably stronger. Thus, we conclude that the equilibrium response to an increase in CO_2 seems somewhat model dependent, although our model's recovery to a somewhat weakened state is at least partially a consequence of our Arctic river runoff modification.

Note that in Figure 5b the dark blue curve (this run's parameter choices are shown by the black star on Figure 4) seems to have stabilized at an intermediate state characterized by weak overturning. Ultimately this run does collapse after 6000 years (the blue curve in Figure 9c), behaving as if it were an unstable equilibrium, *i.e.* a threshold or bifurcation point determining whether the circulation recovers or collapses (in this manuscript we refer to this phenomenon as a bifurcation given that our results seems so well captured by simple non-linear system behavior, although we caution the reader that we have not shown this rigorously). Other runs are further along toward collapse by year 1000; in fact, for the two runs with strongest forcing, high-latitude sinking in the North Atlantic has completely ceased. The monotonic increase of SAT toward an equilibrium value is not affected by a collapse in the ocean circulation, except a very slight yet noticeable decrease in the highest curves in Figure 5a in the last several hundred years (this is caused by an increase in sea-ice extent in the North Atlantic in response to a decrease in the heat transport by the Atlantic branch of the MOC). Thus, despite a profound shift in the large-scale ocean circulation pattern in those runs that collapse, there is only minimal immediate impact on (global mean) SAT.

The decrease in overturning in the first 100 years, like that of SAT, is largely dictated by the rate of CO_2 forcing increase. This is illustrated in **Figure 6**a. The trend is approximately linear for all data points, whether the circulation is ultimately on a path to recovery or collapse (as indicated by the color of data points, showing the overturning strength at year 1000). While the higher CO_2 runs are more favored to collapse by year 1000 (blue points), it is also clear that climate sensitivity plays a role in determining the final outcome. Note that several runs recover despite a high CO_2 concentration (*i.e.* there are several orange and yellow recovering runs amidst the area dominated by blue/collapsing runs), and these too obey the general trend. Conversely, Figure 6b suggests no systematic relationship between the climate sensitivity and overturning strength at year 100.

As illustrated in **Figure 7**, we are able to determine the critical parameter combination that determines whether a collapse occurs in our model: S*Log(C/C_o), the product of climate sensitivity and the logarithm of the multiplicative change in CO_2. All runs which cross a threshold of approximately 7 Sv ultimately collapse; this occurs for S*Log(C/C_o) of approximately 0.8 or higher.

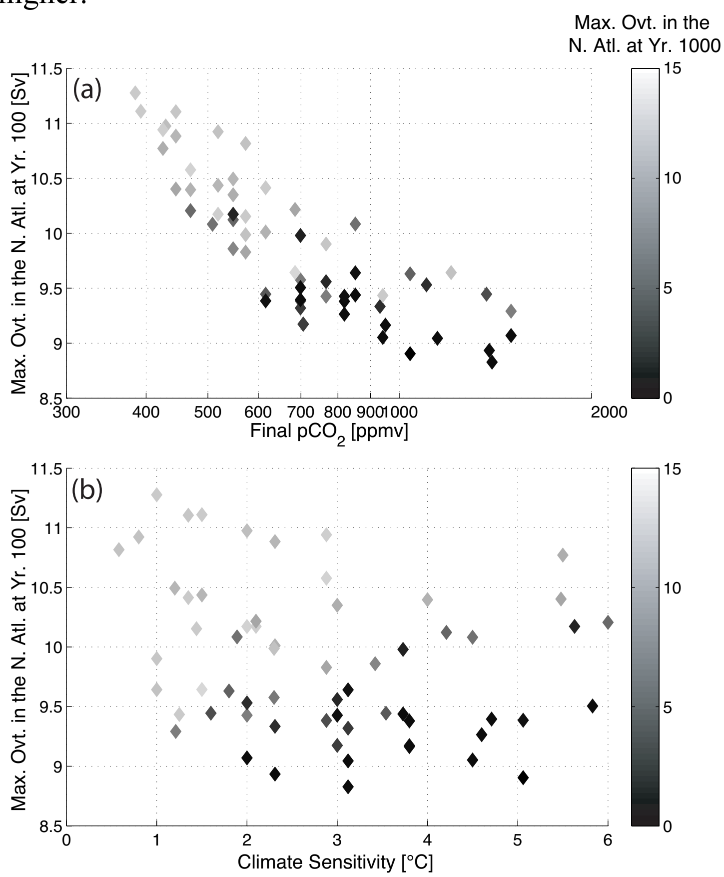

Figures 6. Results for runs with forcings given by the black symbols in Figure 4: **(a)** a maximum overturning streamfunction in the North Atlantic at year 100, *i.e.* at the end of the increase in CO_2 forcing, versus the final concentration of CO_2. The shading of the individual diamonds shows the overtuning at year 1000; dark points indicate a THC collapse; **(b)** same except the overturning is shown versus climate sensitivity.

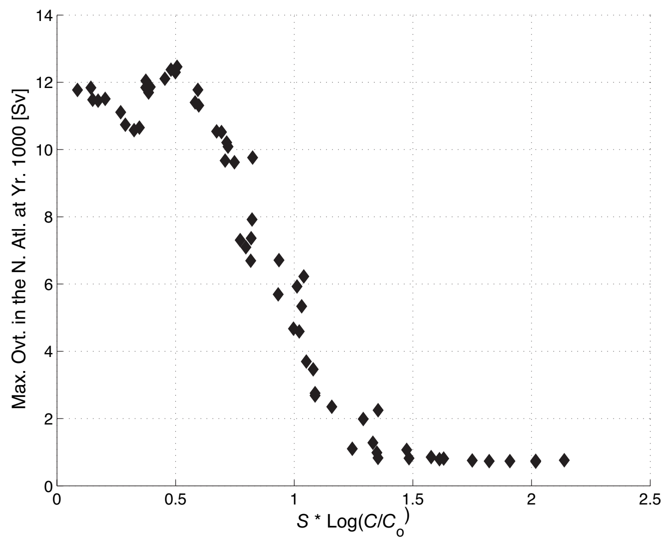

Figure 7. Plot of climate sensitivity times Log(C/C_o) vs. the maximum in North Atlantic overturning streamfunction at year 1000.

Note that this product is proportional to the expected equilibrium increase in SAT; given that all forcing increases occur over 100 years, this product is also linearly proportional to the product of the rate of CO_2 increase and the climate sensitivity. However, it is worth noting that our expected equilibrium increase in SAT does not exactly equal the actual increase in SAT, given that our climate sensitivity was estimated using a mixed layer ocean model (see section 2). Curiously, if one uses the actual climate sensitivity for the run (as estimated from SAT at year 1000), it is no longer possible to define the bifurcation curve in terms of the simple parameter combination. Thus, it would seem that S*Log(C/C_o) is useful to assess stability only if S is defined *without* including the non-linear climate feedback provided by changes in the ocean circulation.

In order to divide phase space into collapsing and recovering regions in Figure 4, we used the parameters for the dark blue run shown in Figure 5 (*i.e.* the run seemingly attracted to an unstable intermediate state) to calculate the critical value of S*Log(C/C_o). Other runs situated very near this "bifurcation curve" may recover or collapse, although as mentioned it often takes many additional hundreds or even thousands of years to determine their ultimate fate (given that our methods are only able to prescribe the model's desired climate sensitivity to within 0.2 °C, this curve should be viewed as approximate; we will show other runs seemingly situated precisely on the curve that just barely recover). Based on SS97 model results, Keller *et al.* (2004) constructed a similar plot of phase space (their Figure 1a), also with a curve separating recovery from collapse. However, they expressed this curve using an empirical fit, in contrast with the simple product of parameters found here. A comparison of these similar plots suggests that our model is somewhat less stable than SS97's model for runs with high climate sensitivities, and considerably less stable for low sensitivity.

The significance of this product goes beyond merely predicting whether the ocean circulation will ultimately collapse or recover; it also can be used to predict the strength of the overturning circulation at year 1000 (Figure 7). The fact that all runs here fall on a well-defined curve suggests two important points: 1) during a collapse, where the climate system is undergoing a fairly dramatic upheaval, the changes in overturning are predictable and well-behaved, despite the chaotic nature of the system; and 2) the overturning circulation behavior is strongly linked to the equilibrium change in SAT. The largest scatter in Figure 7 occurs where the product is small; after recovery most runs seemed to "overshoot" the new equilibrium to some degree, with some of the runs embarking on long-period oscillations (*e.g.*, see Fig 11a).

To illustrate better the respective roles of climate sensitivity and greenhouse gas forcing in governing the response of the MOC, in **Figure 8** we show the North Atlantic overturning strength for runs given by blue and red symbols in Figure 4. The red runs are characterized by a low CO_2 forcing increase and high climate sensitivity, using parameter choices that straddle the bifurcation curve. Conversely, we have chosen the blue runs to have a high level of forcing but low climate sensitivity. Note that these runs are all fairly close to the bifurcation curve, and the product of rate and sensitivity is roughly the same for the recovering runs on both extremes of phase space (the same is true for the collapsing runs). Given the difference in forcing rate between these simulations, there is a noticeable disparity in the change in overturning during the first 100 years, with less decrease exhibited in the slow forcing runs. After 100 years, the low sensitivity forcing pairs almost immediately split apart: the "recovering" runs stop decreasing and meander over the next 100 years before increasing more monotonically, whereas the "collapsing" runs continue to weaken unabated. In contrast, all of the high sensitivity runs meander for an additional 300 years. Thereafter, the collapsing runs begin a steady decrease, and the recovering runs trend back to original strength.

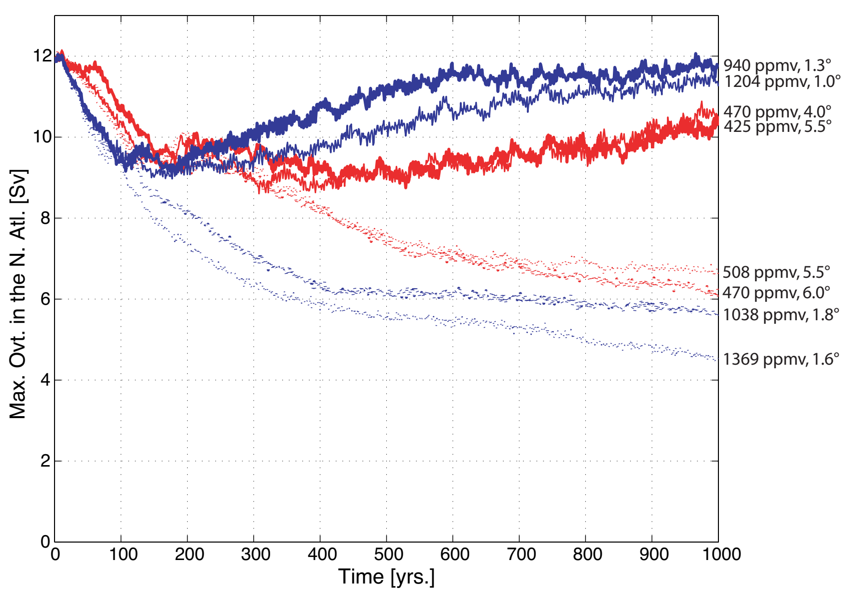

Figure 8. Comparison of the North Atlantic maximum overturning streamfunction for the blue and red runs in Figure 4. The blue time series are high CO_2, low sensitivity runs, and the red curves are low CO_2, high sensitivity runs.

4. DEPENDENCE ON RATE OF CO_2 INCREASE

In this section we shift our focus to how the rate of CO_2 increase affects results, given stabilization at a predetermined level of CO_2. More specifically, we seek to address the following questions: How does the rate of forcing affect runs that collapse? How does rate affect runs that recover? To answer these questions, we use similar parameter choices as runs examined in section 3, but repeat these simulations with either the full change in CO_2 applied at the run outset, or reduce the rate of increase so that the full forcing is not achieved until year 200, year 400, and/or year 1000. A related critical question to be gleaned here is whether rate affects whether a run recovers or collapses; the answer will be discussed more fully in section 5, where it is contrasted with SS97's conclusion.

In the following sub-sections, we first examine additional simulation(s) with parameter choices far from the bifurcation curve (*i.e.* strong forcing runs and weak forcing runs, respectively) and progress to runs closer to the curve. In other words, we begin with forcing scenarios that are presumed to capture the behavior typical over much of phase space, and proceed to special cases either on the threshold of collapse or just barely collapsing. Another objective of our run selection criteria was to ensure testing both high-sensitivity/low CO_2 combinations and vice-versa; unless specifically noted, results were generally similar.

4.1. How does rate affect runs that collapse?

The response in overturning streamfunction for a select run with strong forcing (the black triangle in Figure 4) is shown in **Figure 9**a, for immediate, 100-year, and 1000-year increases in CO_2. The overturning in the immediate forcing run weakens more quickly than when increased over 100 years, as would be expected; after 100 years, this run has decreased to about 7 Sv, whereas the 100 year forcing run has decreased to 9 Sv. All told, however, there is very little difference between the two time series, except for the immediate forcing run leading the 100 year forcing run by approximately 70 years. The overturning collapse in the 1000-year forcing run takes considerably longer to occur. In the first 500 years, the overturning weakens slowly, stabilizing briefly between years 350 and 600, before collapsing monotonically thereafter. The lag between this run and the immediate forcing run is approximately 700 years, which is also the time required for CO_2 to reach its critical level as given by the curve in Figure 4. This qualitative relationship was observed for several other runs in the "collapse" portion of phase space (not shown), both for low and high climate sensitivities. With more marginally unstable runs, however, the lag in collapse was sometimes attenuated further in the 1000-year forcing scenario.

For special cases closer to the bifurcation curve, however, we found several instances where the CO_2 forcing rate does affect the stability behavior. For runs that just barely collapse (given a forcing increase over 100 years), in a few instances we found that rate could affect whether a collapse occurs, as shown in Figures 9b-c. Here, in addition to plotting forcing increases over immediate, 100 years, and 1000 years, we show forcing increases over 200 and 400 years. The forcing in the experiment shown in Figure 9b places it just slightly away from the bifurcation curve (the red square in Figure 4), whereas the parameter combination for the Figure 9c was that

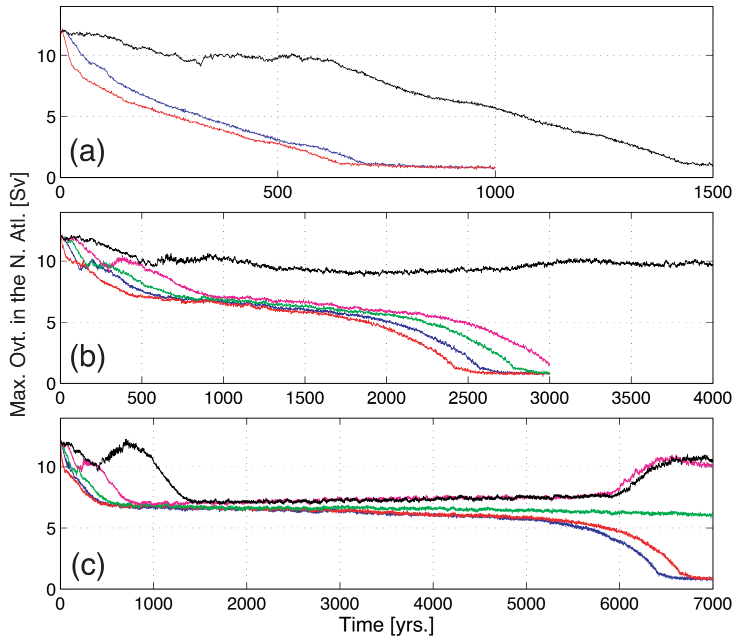

Figures 9. Comparison of North Atlantic maximum overturning streamfunction for select strongly forced runs, all of which collapse when the forcing increase is applied over a 100-year period. CO_2 increases occur instantly (red), over 100 years (blue), 200 years (green), 400 years (magenta), and 1000 years (black): **(a)** located far from the bifurcation curve, 1398 ppmv/2.31° (black triangle in Figure 4); **(b)** close to the bifurcation curve, 509 ppmv/4.5° (red square); **(c)** falling on the bifurcation curve, 856 ppmv/1.9° (black star). Note the change in time scale between subplots.

used to define the curve (the black star in Figure 4; the blue time series is the same both here and in Figure 5). In the former, the 1000-year forcing run does not collapse, whereas in the latter, neither the 1000-year or 400-year forcing runs collapse.

On closer inspection, there are some additional differences between the respective series shown in Figures 9b-c. The 1000-year run in Figure 9b never experiences sufficient weakening to attract it to the unstable intermediate state, whereas all runs in Figure 9c, including the 1000-year and 400-year runs that ultimately recover, remain in this weakened state for several thousand years. The runs that do collapse in Figure 9c seem to show slightly greater weakening prior to reaching this state. Note that the immediate run here actually collapses about a hundred years *after* the 100-year forcing run, although the 200-year run has not even fully collapsed by year 7000; these differences in the time it takes to collapse are inconsistent with our earlier results, presuming the system maintains some "memory" of the overturning strength upon reaching the unstable state. As a further test, we repeated the 400-year forcing run with trivially different initial conditions, and the time series had not yet upturned (as does the 400-year forcing run shown) by the end of the 7000-year simulation. One final observation is that in Figure 9c the overturning in the 1000-year forcing run rebounds during years 400-700, despite increasing CO_2 levels during this period (the same behavior is also evident in the 200- and 400-year forcing runs, to lesser degree, earlier in their respective time series); this would seem to indicate the forcing is sufficiently slow as to allow the recovery mechanism to begin to occur, but ultimately cannot keep pace with the continued rise in CO_2.

Our conclusions from this set of experiments are as follows. For most of the “collapse” portion of phase space, the rate of forcing has little affect on the stability behavior; a slower rate merely delays the response until a critical level of CO_2 forcing is surpassed. However, slower forcing may avoid weakening the overturning to the unstable state, but only if the final forcing is close to the bifurcation curve in Figure 4. For runs that are very close to the bifurcation curve, even very slow forcing may not be sufficient to avoid getting “stuck” in the weak unstable state for several thousand years. We also speculate that the chaotic nature of the system might affect whether the overturning ultimately collapses or recovers given a final forcing precisely at the bifurcation curve (in addition to affecting the time to recovery or collapse), although further (CPU-intensive) testing would be needed to confirm this hypothesis.

4.2. How does rate affect runs that recover?

In **Figure 10** we show two sets of experiments with relatively weak final CO_2 forcing, given immediate, 100- and 1000-year forcing periods. In the bottom panel (the run is given by the black circle in Figure 4) the nadir in overturning is slightly greater in the immediate forcing run than the 100-year run although the opposite is true in the top panel (the black square in Figure 4). Except for these minor differences in the initial few hundred years, in both panels the immediate and 100-year forcing runs are quite similar to each other. Given a rapid increase in forcing, the time scale to reach the minimum in overturning is order 100 years, even with the immediate forcing runs. As such, the 100-year forcing run in Figure 10b (low climate sensitivity) exhibits its minimum at about the same time as the immediate forcing run, although it takes slightly longer for the 100-year forcing run to reach its minimum in Figure 10a (medium climate sensitivity). Thus, there appears to be an internal ocean timescale which constrains how fast the

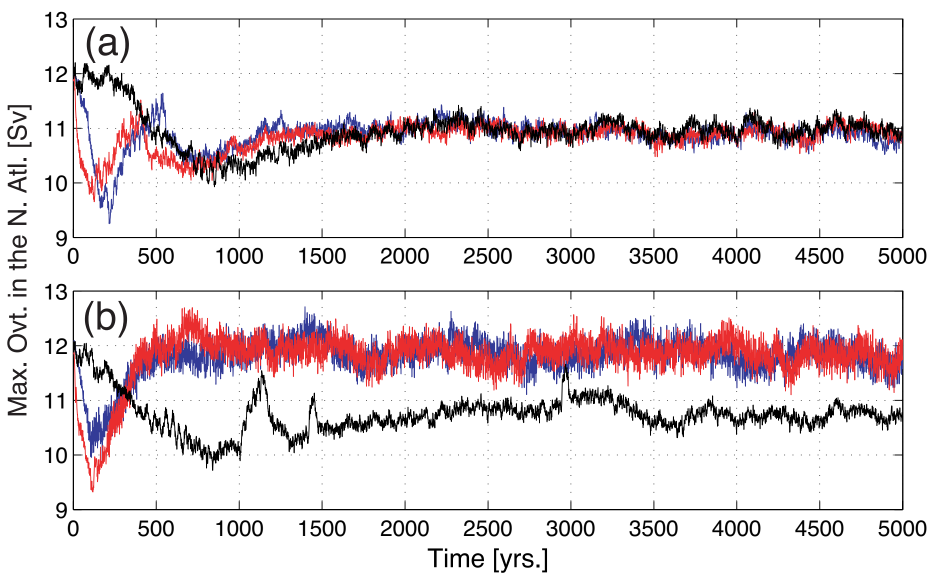

Figures 10. Comparison of North Atlantic maximum overturning streamfunction for select weakly forced runs; when forcing increases are applied over a 100-year period, these runs are characterized by a rapid recovery. CO_2 increases occur instantly (red), over 100 years (blue), and over 1000 years (black): **(a)** 446 ppmv/2.31° (black square in Figure 4); **(b)** 617 ppmv/1.35° (black circle).

system can respond to instant CO_2 changes, and unless the climate sensitivity is high (which as discussed, delays the effective response), there is little practical difference between increasing the forcing as a step-function or more gradually increasing forcing over a centennial time scale.

When forcing increases occur over a 1000-year period, in both panels of Figure 10 the maximum weakening in overturning is roughly the same as in simulations with more rapidly forcing increases. This suggests that for our weakly forced runs, the maximum weakening is not affected by the rate at which the forcing increase occurs, a result also noted in SM99's study. During the 1000-year period of forcing increase, overturning decreases fairly uniformly, with recovery ensuing once the forcing is held constant. Curiously, in Figure 10b, the time series remains at a lower overturning, whereas in Figure 10a both series converge by year 2000 (although it appears in Figure 10b the 100- and 1000-year series might ultimately converge if integrated for additional millennia). The reason for the behavior is unclear; in our longer-term runs, the parameter choice used in Figure 10b was the only one to exhibit different recovery equilibria given identical final CO_2 forcing levels. Thus, we conclude that even 1000-year forcing is not sufficiently slow to maintain quasi-equilibrium, given a change in the magnitude of CO_2 on the order of doubling. This observation was also noted by SM99, and based on the supporting physical argument of slow adjustment timescales in the ocean (particularly, vertical diffusion), would seem to be model-independent.

In **Figure 11** we show similar time series for two runs closer to the bifurcation curve (the red circle and blue triangle in Figure 4, respectively). Again there is little difference between the immediate and 100-year forcing runs, although the disparity in the rate of the initial decline is greater in Figure 11a, owing to the high sensitivity of this run. There are several other interesting behaviors seen in these runs, specifically the long-term oscillation in Figure 11a and the marked

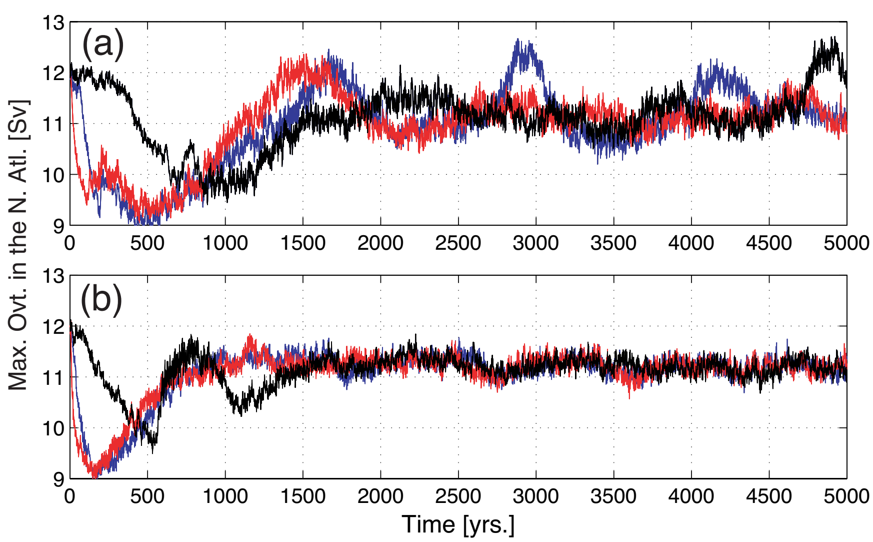

Figures 11. Comparison of North Atlantic maximum overturning streamfunction for select weakly forced runs; as in Fig 10, these runs all recover when forcing increases are applied over 100 years, although the forcing is somewhat stronger here and the recovery somewhat slower. CO_2 increases occur instantly (red), over 100 years (blue), and over 1000 years (black): **(a)** 425 ppmv/5.5° (red circle in Figure 4); **(b)** 1215 ppmv/1.0° (blue triangle).

increase in overturning during years 500-700 of the 1000-year forcing run in Figure 11b (similar to that discussed in Figure 9c). Also worth noting is that the maximum decrease in overturning for the 1000-year forcing runs is now noticeably less than for more rapidly forced time series.

The effect of slower forcing is even more noticeable for the special case of several parameter combinations that fell nearly exactly on our bifurcation curve, as shown in **Figure 12** (runs given by the green symbols in Figure 4). Here, only the immediate and 100-year forcing runs decrease sufficiently to reach the proximity of the unstable intermediate state; the minimal decrease in overturning for the 1000-year forcing runs is especially apparent in Figure 12b-c. In Figure 12b, we show the only occurrence where immediate forcing had any significant effect in comparison with 100-year forcing; this run gets "caught" at the intermediate state for several thousand years. In Figure 12c, the recovery process is particularly sluggish, despite low climate sensitivity, with even the 1000-year run continuing to decrease well after the forcing is held constant. The "recovery" state exhibited by this forcing/sensitivity combination exhibited the weakest overturning of any experiment, approximately 20% shy of the original strength.

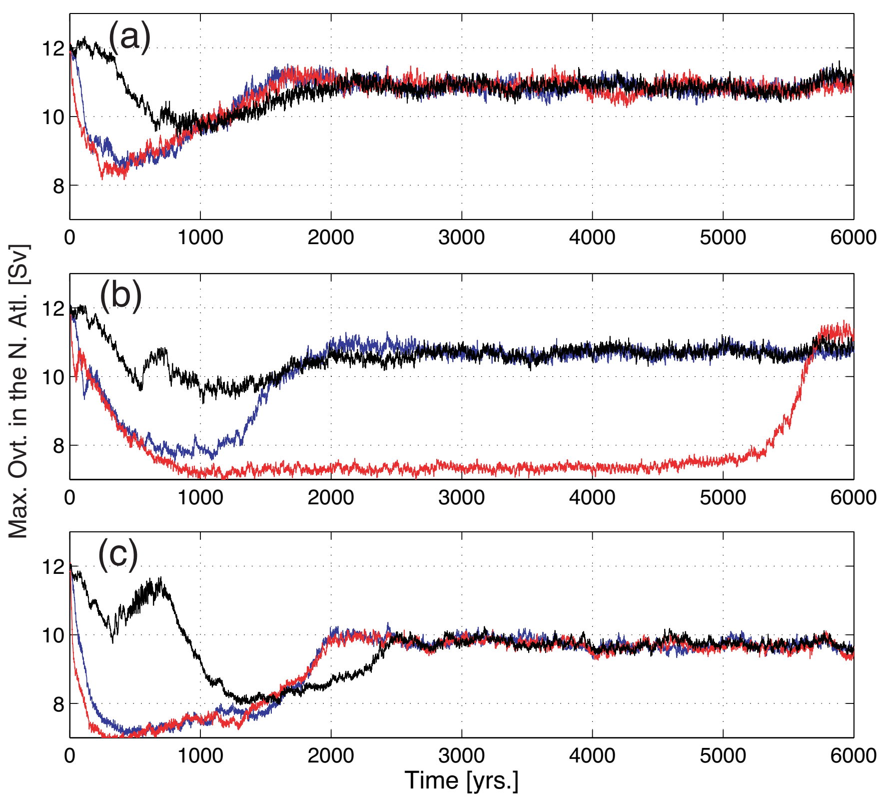

Figures 12. Comparison of North Atlantic maximum overturning streamfunction for three special cases of marginally stable runs (*i.e.* located on the bifurcation curve) given forcing over 100 years. CO_2 increases occur instantly (red), over 100 years (blue), and over 1000 years (black): **(a)** 446 ppmv/5.48° (green square in Figure 4); **(b)** 548 ppmv/3.42° (green circle); **(c)** 1514 ppmv/1.21° (green triangle).

5. SUMMARY AND DISCUSSION

In this work we have run many simulations of our coupled model of intermediate complexity, effectively mapping phase space for two uncertain parameters, the level of forcing increase and climate sensitivity.

We find that changes in SAT equilibrate within a few centuries, at a level proportional to the product of the radiative forcing and the climate sensitivity. This product also determines whether the ocean circulation collapses across our phase space, hence the obvious conclusion is that MOC weakening is a direct response to SAT increases. However, it is not simply changes in the air-sea heat flux that cause the changes in overturning; using a more evenly distributed river runoff scheme (*i.e.* rather than dumping anomalous runoff where it is most effective in weakening the MOC), the model's ocean circulation did not collapse for a sampling of runs across phase space. Hence, the collapse is a result of climate feedbacks, particularly increases in freshwater forcing, as the SAT increases. These results stress the need for continued observations of Arctic river discharge. Although this model is highly idealized, it demonstrates that the circulation could be quite susceptible to collapse, given a relatively minor change in freshwater forcing, as long as this change impacts a location of dynamical significance.

We find that for marginally stable parameter combinations of final CO_2 and climate sensitivity (*i.e.* those runs which are situated near our bifurcation curve), the rate of forcing can affect whether a collapse occurs. Lucarini *et al.* (2005) explain the behavior noted here; they used a single hemisphere, 2D ocean model, and thus were able to analyze the behavior more rigorously. Specifically, they found a separation between fast and slow regimes of forcing. An internal ocean advective timescales of several hundred years determines this separation. For sufficiently slow forcing, the system is able to begin to equilibrate through advective adjustment, permitting some runs to recover that would collapse given a more rapid forcing. Given the importance of these slow internal ocean timescales, there is less practical difference when forcing occurs over periods much shorter than this advective time scale.

However, for the majority of our runs across phase space, we find that the rate of forcing increase has little effect on the stability of the circulation; only several runs situated near the bifurcation curve proved to be exceptions. This result is in striking contrast with SS97's results, where the implication was that rate is very important across all of phase space, as implied by their Figure 4. For example, for a climate sensitivity of 3.7°C, their Figure 4 suggests that the critical CO_2 concentration ranges from approximately 950 ppmv (forcing increases occurring over a 625 year period) to 630 ppmv (forcing increases over 40 years). Similarly, for a lower climate sensitivity of 2.6°C, the range is 1600 ppmv (880 years) to 900 ppmv (60 years). A closer examination of SS97's Figure 4 shows that the isopleths of critical CO_2 have finite slopes all through phase space (in this figure, no rate dependence would result in vertical isopleths). These slopes tend to flatten further for low rates of increase, which not coincidentally is where the time of forcing increase approaches the ocean advective timescale. As discussed in section 1, 2D models lack many important features of the ocean circulation, and thus we would suggest that these missing elements, operating on faster timescales than large-scale advection, play an important role in transient forcing experiments. It would seem that by including these faster processes, our model is rather insensitive to a forcing increase occurring over different periods under 100 years, which are typical timescales that could conceivable be of interest for greenhouse gas policy discussions.

Climate feedbacks operate more slowly for high sensitivity runs than low sensitivity runs. Therefore, further increases in SAT during the centuries after CO_2 stabilization were more significant in high sensitivity runs. Since the response in MOC is ultimately governed by these increases, the processes of weakening and collapse or recovery also operate more slowly in high sensitivity runs. There was minimal change in global mean SAT as the circulation collapsed, despite a complete reorganization of the oceans' large-scale circulation pattern. We find that the collapse in our model operates on a slow timescale and is well behaved, such that it was possible to closely predict the MOC's weakening at year 1000 given an experiment's parameter combination. In this model, deep sinking initiates in the North Pacific. This Atlantic-Pacific "seesaw" behavior has been observed in at least one other model (Saenko *et al*., 2004), although not specifically in the context of global warming experiments.

It is worth noting that the behavior of the global ocean circulation in this coupled model is like a simple bifurcation, lending credibility to box model studies of the interhemispheric ocean circulation, such as those described in Rahmstorf (1996), Scott *et al*. (1999), Gregory *et al*. (2003), and Lucarini and Stone (2005). Of particular relevance to policy-makers is that for some parameter combinations the ocean circulation seems predestined to collapse in several centuries, albeit with only modest immediate change in the MOC; moreover, in some cases it took several centuries (or more) to distinguish between similar runs that eventually collapsed and those that recovered.

Acknowledgements

The authors thank Stephanie Dutkiewicz for assistance with the coupled model and for numerous helpful comments and discussions. This research was supported in part by the Methods and Models for Integrated Assessments Program of the National Science Foundation, Grant ATM-9909139, by the Office of Science (BER), U.S. Department of Energy, Grant No. DE-FG02-93ER61677, and by the MIT Joint Program on the Science and Policy of Global Change (JPSPGC). Financial support does not constitute an endorsement by NSF, DOE, or JPSPGC of the views expressed in this article.

6. REFERENCES

Andronova NG, Schlesinger ME (2001) Objective estimation of the probability density function for climate sensitivity. *J Geophys Res,* **106**: 22,605-22,612.

Bitz CM, Lipscombe WH (1999) An energy-conserving thermodynamic model of sea ice. *J Geophys Res,* **104**: 15,669-15,677.

Colman R (2003) A comparison of climate feedbacks in general circulation models. *Clim Dyn,* **20**: 865-873.

Cubasch *et al*. (2001) Projections of future climate change. In: J. T. Houghton *et al*. (eds) *Climate Change 2001: The Scientific Basis: Contribution of Working Group I to the Third Assessment Report of the Intergovernmental Panel on Climate Change*. Cambridge Univ. Press, New York, pp. 525-582.

Dutkiewicz S, Sokolov A, Scott JR, Stone PH (2005) A three-dimensional ocean-sea-ice-carbon cycle model and its coupling to a two-dimensional atmospheric model: uses in climate change studies, Joint Program on the Science and Policy of Global Change *Report 122*, MIT, Cambridge, MA.

Forest CE, Stone PH, Sokolov AP, Allen MR, Webster M (2002) Quantifying uncertainties in climate system properties with the use of recent climate observations. *Science,* **295**: 113-117.

Forest CE, Stone PH, Sokolov AP (2006) Estimated PDFs of climate system properties including natural and anthropogenic forcings. *Geophys Res Lett,* **33**: L10705. DOI 10.1029/2005GL023977.

Ganachaud A, Wunsch C (2000) The oceanic meridional overturning circulation, mixing, bottom water formation and heat transport. *Nature,* **408**: 453-457.

Gent P, McWilliams J (1990) Isopycnal mixing in ocean circulation models. *J Phys Oceanogr,* **20**: 150-155.

Goosse H, Fichefet T, Campin J-M (1997) The effects of the water flow through the Canadian Archipelago in a global ice-ocean model. *Geophys Res Lett*, **24**: 1507-1510.

Gregory, JM *et al*. (2005) A model intercomparison of changes in the Atlantic thermohaline circulation in response to increasing atmospheric CO_2 concentration. *Geophys Res Lett,* **32**: L12703. DOI 10.1029/2005GL023209.

Gregory JM, Saenko OA, Weaver AJ (2003) The role of the Atlantic freshwater balance in the hysteresis of the meridional overturning circulation. *Clim Dyn* **21**: 707-717.

Gregory JM, Stouffer RJ, Raper SCB, Stott PA, Rayner NA (2002) An observationally based estimate of the climate sensitivity. *J Clim,* **15**: 3117-3121.

Hansen J, Russell G, Lacis A, Fung I, Rind D, Stone P (1985) Climate response times: dependence on climate sensitivity and ocean mixing. *Science,* **229**: 857-859.

Hansen J, Russell G, Rind D, Stone P, Lacis A, Lebedeff S, Ruedy R, Travis L (1983) Efficient three-dimensional global models for climate studies: Models I and II. Mon Weather Rev 111: 609-662.

Huang B, Stone PH, Sokolov AP, Kamenkovich IV (2003) The deep-ocean heat uptake in transient climate change. *J Clim,* **16**: 1352-1363.

Jiang S, Stone PH, Malanotte-Rizzoli P (1999) An assessment of the GFDL ocean model with coarse resolution. Part I: annual-mean climatology. *J Geophys Res,* **104**: 25,623-25,646.

Kamenkovich IV, Marotzke J, Stone PH (2000) Factors affecting heat transport in an ocean general circulation model. *J Phys Oceanogr,* **30**: 175-194.

Kamenkovich IV, Sokolov AP, Stone PH (2002) An efficient climate model with a 3D ocean and statistical-dynamical atmosphere. *Clim Dyn,* **19**: 585-598.

Keller K, Bolker BM, Bradford DF (2004) Uncertain climate thresholds and optimal economic growth. *J Envir Econ Manage,* **48**: 723-741.

Levitus S, Boyer TP (1994) *World Ocean Atlas 1994 Volume 4: Temperature, NOAA Atlas NESDIS 4*, U.S. Department of Commerce, Washington, D.C., 117pp.

Lucarini V, Calmanti S, Artale V (2005) Destabilization of the thermohaline circulation by transient changes in the hydrological cycle. *Clim Dyn,* **24**: 253-262.

Lucarini V, Stone PH (2005) Thermohaline circulation stability: a box model study. Part II: coupled atmosphere-ocean model. *J Clim,* **18**: 514-529.

Marshall J, Adcroft A, Hill C, Perelman L, Heisey C (1997) A finite-volume, incompressible Navier-Stokes model for studies of the ocean on parallel computers. *J Geophys Res,* **102**: 5753-5766.

Marotzke J, Scott JR (1999) Convective mixing and the thermohaline circulation. *J Phys Oceanogr,* **29**: 2962-2970.

Marotzke J, Stone PH (1995) Atmospheric transports, the thermohaline circulation, and flux adjustments in a simple coupled model. *J Phys Oceanogr,* **25**: 1350-1364.

Meehl GA, Washington WM, Arblaster JM, Hu A (2004) Factors affecting climate sensitivity in global coupled models. *J Clim,* **17**: 1584-1596.

Otterå OH, Drange H, Bentsen M, Kvamsto NG, Jiang D (2004) Transient response of the Atlantic Meridional Overturning Circulation to enhanced freshwater input to the Nordic Seas-Arctic Ocean in the Bergen Climate Model. *Tellus,* **A 56**: 342-361.

Peltier WR, Vettoretti G, Stastnsa M (2006) Atlantic meridional overturning and climate response to Arctic Ocean freshening. *Geophys Res Lett,* **33**: L06713. DOI 10.1029/2005GL025251.

Peterson BJ, Holmes RM, McClelland JW, Vorosmarty CJ, Lammers RB, Shiklomanov AI, Shiklomanov IA, Rahmstorf S (2002), Increasing river discharge into the Arctic Ocean. *Science* , **298**: 2171-2173.

Raper SCB, Gregory JM, Stouffer RJ (2002) The role of climate sensitivity and ocean heat uptake on AOGCM transient temperature response. *J Clim,* **15**: 1584-1596.

Rahmstorf S (1996) On the freshwater forcing and transport of the Atlantic thermohaline circulation. *Clim Dyn,* **12**: 799-811.

Rahmstorf S, Crucifix M, Ganopolski A, Goosse H, Kamenkovich I, Knutti R, Lohmann G, Marsh B, Mysak L, Wang Z, Weaver A (2005) Thermohaline circulation hysteresis: A model intercomparison. *Geophys Res Lett,* **32**: L23605. DOI 10.1029/2005GL023655.

Rennermalm AK, Wood EF, Déry SJ, Weaver AJ, Eby M (2006) Sensitivity of the thermohaline circulation to Arctic Ocean runoff. *Geophys Res Lett,* **33**: L12703. DOI 10.1029/2006GL026124.

Redi MH (1982) Oceanic isopycnal mixing by coordinate rotation. *J Phys Oceanogr,* **12**: 1154-1158.

Saenko OA, Schmittner A, Weaver AJ (2004) The Atlantic-Pacific seesaw. *J Clim*, **17**: 2033-2038.

Schmittner A, Stocker TF (1999) The stability of the thermohaline circulation in global warming experiments. *J Clim,* 12: 1117-1133.

Scott JR, Marotzke J, Stone PH (1999) Interhemispheric thermohaline circulation in a coupled box model. *J Phys Oceanogr,* **29**: 351-365.

Sokolov A, Stone PH (1998) A flexible climate model for use in integrated assessments. *Clim Dyn,* **14**: 291-303.

Stocker TF, Schmittner A (1997) Influence of CO_2 emission rates on the stability of the thermohaline circulation. *Nature,* **388**: 862-865.

Stouffer RJ, Manabe S (1999) Response of a coupled ocean-atmosphere model to increasing atmospheric carbon dioxide: Sensitivity to the rate of increase. *J Clim,* **12**: 2224-2237.

Stouffer RJ, Manabe S (2003) Equilibrium response of thermohaline circulation to large changes in atmospheric CO_2 concentration. *Clim Dyn,* **20**: 759-773.

Talley LD, Reid JL, Robbins PE (2003) Data-based meridional overturning streamfunctions for the global ocean. *J Clim,* **16**: 3213-3226.

Trenberth K, Olson J, Large W (1989) A global wind stress climatology based on ECMWF analyses, *Tech. Rep. NCAR/TN-338+STR*, National Center for Atmospheric Research, Boulder, Colorado.

Webster MD, Babiker M, Mayer M, Reilly JM, Harnisch J, Sarofim MC, Wang C (2002) Uncertainty in emissions projections for climate models. *Atmos Envir,* **36**: 3659-3670.

Weijer W, Dijkstra HA (2001) A bifurcation study of the three-dimensional thermohalince ocean circulation: The double hemisphere case. *J Mar Res,* **33**: 599-631.

Wiebe EC, Weaver AJ (1999) On the sensitivity of global warming experiments to the parametrisarion of sub-grid scale ocean mixing. *Clim Dyn*, **15**: 875-893.

Winton M (2000) A reformulated three-layer sea ice model. *J Atmos Ocean Tech,* **17**: 525-531.

Wright DG, Stocker TF, Mercer D (1998) Closure used in zonally averaged models, *J Phys Oceanogr,* **28**: 791-804.

Wu P, Wood R, Stott P (2005) Human influences on increasing Arctic river discharges. *Geophys Res Lett*, **32**: L02703. DOI 10.1029/2004GL021570.

REPORT SERIES of the **MIT** ***Joint Program on the Science and Policy of Global Change***

1. **Uncertainty in Climate Change Policy Analysis** *Jacoby & Prinn* December 1994
2. **Description and Validation of the MIT Version of the GISS 2D Model** *Sokolov & Stone* June 1995
3. **Responses of Primary Production and Carbon Storage to Changes in Climate and Atmospheric CO_2 Concentration** *Xiao et al.* October 1995
4. **Application of the Probabilistic Collocation Method for an Uncertainty Analysis** *Webster et al.* January 1996
5. **World Energy Consumption and CO_2 Emissions: 1950-2050** *Schmalensee et al.* April 1996
6. **The MIT Emission Prediction and Policy Analysis (EPPA) Model** *Yang et al.* May 1996 (superseded *by No. 125*)
7. **Integrated Global System Model for Climate Policy Analysis** *Prinn et al.* June 1996 (superseded *by No. 124*)
8. **Relative Roles of Changes in CO_2 and Climate to Equilibrium Responses of Net Primary Production and Carbon Storage** *Xiao et al.* June 1996
9. **CO_2 Emissions Limits:** ***Economic Adjustments and the Distribution of Burdens*** *Jacoby et al.* July 1997
10. **Modeling the Emissions of N_2O and CH_4 from the Terrestrial Biosphere to the Atmosphere** *Liu* Aug. 1996
11. **Global Warming Projections:** ***Sensitivity to Deep Ocean Mixing*** *Sokolov & Stone* September 1996
12. **Net Primary Production of Ecosystems in China and its Equilibrium Responses to Climate Changes** *Xiao et al.* November 1996
13. **Greenhouse Policy Architectures and Institutions** *Schmalensee* November 1996
14. **What Does Stabilizing Greenhouse Gas Concentrations Mean?** *Jacoby et al.* November 1996
15. **Economic Assessment of CO_2 Capture and Disposal** *Eckaus et al.* December 1996
16. **What Drives Deforestation in the Brazilian Amazon?** *Pfaff* December 1996
17. **A Flexible Climate Model For Use In Integrated Assessments** *Sokolov & Stone* March 1997
18. **Transient Climate Change and Potential Croplands of the World in the 21st Century** *Xiao et al.* May 1997
19. **Joint Implementation:** ***Lessons from Title IV's Voluntary Compliance Programs*** *Atkeson* June 1997
20. **Parameterization of Urban Subgrid Scale Processes in Global Atm. Chemistry Models** *Calbo et al.* July 1997
21. **Needed: A Realistic Strategy for Global Warming** *Jacoby, Prinn & Schmalensee* August 1997
22. **Same Science, Differing Policies;** ***The Saga of Global Climate Change*** *Skolnikoff* August 1997
23. **Uncertainty in the Oceanic Heat and Carbon Uptake and their Impact on Climate Projections** *Sokolov et al.* September 1997
24. **A Global Interactive Chemistry and Climate Model** *Wang, Prinn & Sokolov* September 1997
25. **Interactions Among Emissions, Atmospheric Chemistry & Climate Change** *Wang & Prinn* Sept. 1997
26. **Necessary Conditions for Stabilization Agreements** *Yang & Jacoby* October 1997
27. **Annex I Differentiation Proposals:** ***Implications for Welfare, Equity and Policy*** *Reiner & Jacoby* Oct. 1997
28. **Transient Climate Change and Net Ecosystem Production of the Terrestrial Biosphere** *Xiao et al.* November 1997
29. **Analysis of CO_2 Emissions from Fossil Fuel in Korea: 1961–1994** *Choi* November 1997
30. **Uncertainty in Future Carbon Emissions:** ***A Preliminary Exploration*** *Webster* November 1997
31. **Beyond Emissions Paths:** ***Rethinking the Climate Impacts of Emissions Protocols*** *Webster & Reiner* November 1997
32. **Kyoto's Unfinished Business** *Jacoby et al.* June 1998
33. **Economic Development and the Structure of the Demand for Commercial Energy** *Judson et al.* April 1998
34. **Combined Effects of Anthropogenic Emissions and Resultant Climatic Changes on Atmospheric OH** *Wang & Prinn* April 1998
35. **Impact of Emissions, Chemistry, and Climate on Atmospheric Carbon Monoxide** *Wang & Prinn* April 1998
36. **Integrated Global System Model for Climate Policy Assessment:** ***Feedbacks and Sensitivity Studies*** *Prinn et al.* June 1998
37. **Quantifying the Uncertainty in Climate Predictions** *Webster & Sokolov* July 1998
38. **Sequential Climate Decisions Under Uncertainty:** ***An Integrated Framework*** *Valverde et al.* September 1998
39. **Uncertainty in Atmospheric CO_2 (Ocean Carbon Cycle Model Analysis)** *Holian* Oct. 1998 (superseded *by No. 80*)
40. **Analysis of Post-Kyoto CO_2 Emissions Trading Using Marginal Abatement Curves** *Ellerman & Decaux* Oct. 1998
41. **The Effects on Developing Countries of the Kyoto Protocol and CO_2 Emissions Trading** *Ellerman et al.* November 1998
42. **Obstacles to Global CO_2 Trading:** ***A Familiar Problem*** *Ellerman* November 1998
43. **The Uses and Misuses of Technology Development as a Component of Climate Policy** *Jacoby* November 1998
44. **Primary Aluminum Production:** ***Climate Policy, Emissions and Costs*** *Harnisch et al.* December 1998
45. **Multi-Gas Assessment of the Kyoto Protocol** *Reilly et al.* January 1999
46. **From Science to Policy:** ***The Science-Related Politics of Climate Change Policy in the U.S.*** *Skolnikoff* January 1999
47. **Constraining Uncertainties in Climate Models Using Climate Change Detection Techniques** *Forest et al.* April 1999
48. **Adjusting to Policy Expectations in Climate Change Modeling** *Shackley et al.* May 1999
49. **Toward a Useful Architecture for Climate Change Negotiations** *Jacoby et al.* May 1999
50. **A Study of the Effects of Natural Fertility, Weather and Productive Inputs in Chinese Agriculture** *Eckaus & Tso* July 1999
51. **Japanese Nuclear Power and the Kyoto Agreement** *Babiker, Reilly & Ellerman* August 1999

Contact the Joint Program Office to request a copy. The Report Series is distributed at no charge.

Contact the Joint Program Office to request a copy. The Report Series is distributed at no charge.

REPORT SERIES of the **MIT** ***Joint Program on the Science and Policy of Global Change***

102. Induced Technical Change and the Cost of Climate Policy *Sue Wing* September 2003
103. Past and Future Effects of Ozone on Net Primary Production and Carbon Sequestration Using a Global Biogeochemical Model *Felzer et al.* (revised) January 2004
104. A Modeling Analysis of Methane Exchanges Between Alaskan Ecosystems and the Atmosphere *Zhuang et al.* November 2003
105. Analysis of Strategies of Companies under Carbon Constraint *Hashimoto* January 2004
106. Climate Prediction: *The Limits of Ocean Models* *Stone* February 2004
107. Informing Climate Policy Given Incommensurable Benefits Estimates *Jacoby* February 2004
108. Methane Fluxes Between Terrestrial Ecosystems and the Atmosphere at High Latitudes During the Past Century *Zhuang et al.* March 2004
109. Sensitivity of Climate to Diapycnal Diffusivity in the Ocean *Dalan et al.* May 2004
110. Stabilization and Global Climate Policy *Sarofim et al.* July 2004
111. Technology and Technical Change in the MIT EPPA Model *Jacoby et al.* July 2004
112. The Cost of Kyoto Protocol Targets: *The Case of Japan* *Paltsev et al.* July 2004
113. Economic Benefits of Air Pollution Regulation in the USA: *An Integrated Approach* *Yang et al.* (revised) Jan. 2005
114. The Role of Non-CO_2 Greenhouse Gases in Climate Policy: *Analysis Using the MIT IGSM* *Reilly et al.* Aug. '04
115. Future U.S. Energy Security Concerns *Deutch* Sep. '04
116. Explaining Long-Run Changes in the Energy Intensity of the U.S. Economy *Sue Wing* Sept. 2004
117. Modeling the Transport Sector: *The Role of Existing Fuel Taxes in Climate Policy* *Paltsev et al.* November 2004
118. Effects of Air Pollution Control on Climate *Prinn et al.* January 2005
119. Does Model Sensitivity to Changes in CO_2 Provide a Measure of Sensitivity to the Forcing of Different Nature? *Sokolov* March 2005
120. What Should the Government Do To Encourage Technical Change in the Energy Sector? *Deutch* May '05
121. Climate Change Taxes and Energy Efficiency in Japan *Kasahara et al.* May 2005
122. A 3D Ocean-Seaice-Carbon Cycle Model and its Coupling to a 2D Atmospheric Model: *Uses in Climate Change Studies* *Dutkiewicz et al.* (revised) November 2005
123. Simulating the Spatial Distribution of Population and Emissions to 2100 *Asadoorian* May 2005
124. MIT Integrated Global System Model (IGSM) Version 2: *Model Description and Baseline Evaluation* *Sokolov et al.* July 2005
125. The MIT Emissions Prediction and Policy Analysis (EPPA) Model: *Version 4* *Paltsev et al.* August 2005
126. Estimated PDFs of Climate System Properties Including Natural and Anthropogenic Forcings *Forest et al.* September 2005
127. An Analysis of the European Emission Trading Scheme *Reilly & Paltsev* October 2005
128. Evaluating the Use of Ocean Models of Different Complexity in Climate Change Studies *Sokolov et al.* November 2005
129. *Future* Carbon Regulations and *Current* Investments in Alternative Coal-Fired Power Plant Designs *Sekar et al.* December 2005
130. Absolute vs. Intensity Limits for CO_2 Emission Control: *Performance Under Uncertainty* *Sue Wing et al.* January 2006
131. The Economic Impacts of Climate Change: *Evidence from Agricultural Profits and Random Fluctuations in Weather* *Deschenes & Greenstone* January 2006
132. The Value of Emissions Trading *Webster et al.* Feb. 2006
133. Estimating Probability Distributions from Complex Models with Bifurcations: *The Case of Ocean Circulation Collapse* *Webster et al.* March 2006
134. Directed Technical Change and Climate Policy *Otto et al.* April 2006
135. Modeling Climate Feedbacks to Energy Demand: *The Case of China* *Asadoorian et al.* June 2006
136. Bringing Transportation into a Cap-and-Trade Regime *Ellerman, Jacoby & Zimmerman* June 2006
137. Unemployment Effects of Climate Policy *Babiker & Eckaus* July 2006
138. Energy Conservation in the United States: *Understanding its Role in Climate Policy* *Metcalf* Aug. '06
139. Directed Technical Change and the Adoption of CO_2 Abatement Technology: *The Case of CO_2 Capture and Storage* *Otto & Reilly* August 2006
140. The Allocation of European Union Allowances: *Lessons, Unifying Themes and General Principles* *Buchner et al.* October 2006
141. Over-Allocation or Abatement? *A preliminary analysis of the EU ETS based on the 2006 emissions data* *Ellerman & Buchner* December 2006
142. Federal Tax Policy Towards Energy *Metcalf* Jan. 2007
143. Technical Change, Investment and Energy Intensity *Kratena* March 2007
144. Heavier Crude, Changing Demand for Petroleum Fuels, Regional Climate Policy, and the Location of Upgrading Capacity: *A Preliminary Look* *Reilly, Paltsev & Choumert* April 2007
145. Biomass Energy and Competition for Land *Reilly & Paltsev* April 2007
146. Assessment of U.S. Cap-and-Trade Proposals *Paltsev et al.*, April 2007
147. A Global Land System Framework for Integrated Climate-Change Assessments *Schlosser et al.* May 2007
148. Relative Roles of Climate Sensitivity and Forcing in Defining the Ocean Circulation Response to Climate Change *Scott et al. May 2007*

Contact the Joint Program Office to request a copy. The Report Series is distributed at no charge.